Thin structured rigid body for acoustic absorption

T. A. Starkey, J. D. Smith, A. P. Hibbins, J. R. Sambles, and H. J. Rance

Citation: Appl. Phys. Lett. **110**, 041902 (2017); doi: 10.1063/1.4974487
View online: http://dx.doi.org/10.1063/1.4974487
View Table of Contents: http://aip.scitation.org/toc/apl/110/4
Published by the American Institute of Physics

Thin structured rigid body for acoustic absorption

T. A. Starkey,[1,a)] J. D. Smith,[2] A. P. Hibbins,[1] J. R. Sambles,[1] and H. J. Rance[1]
[1]*Department of Physics and Astronomy, University of Exeter, Stocker Road, Exeter, Devon EX4 4QL, United Kingdom*
[2]*DSTL, Porton Down, Salisbury, Wiltshire SP4 0JQ, United Kingdom*

(Received 14 November 2016; accepted 23 December 2016; published online 23 January 2017)

We present a thin acoustic metamaterial absorber, comprised of only rigid metal and air, that gives rise to near unity absorption of airborne sound on resonance. This simple, easily fabricated, robust structure comprising a perforated metal plate separated from a rigid wall by a deeply subwavelength channel of air is an ideal candidate for a sound absorbing panel. The strong absorption in the system is attributed to the thermo-viscous losses arising from a sound wave guided between the plate and the wall, defining the subwavelength channel. *Published by AIP Publishing.*
[http://dx.doi.org/10.1063/1.4974487]

A perfect absorber, of deep subwavelength scale, is of great interest to the scientific community and engineers alike in their quest for attenuation of acoustic waves. In recent years, acoustic metamaterials, structures patterned on a subwavelength scale that exhibit novel properties not observed in nature for the control of sound, have been the focus of research interest. Pioneering work investigating these exotic structures has led to new ideas and concepts for the attenuation of low-frequency airborne sound, challenging the performance of more traditional structures such as those utilising fibrous or porous materials[1] or micro-perforated panels.[2]

These novel structures that include membrane-type acoustic metamaterials, which in general consist of an elastic membrane supported by a rigid grid and "decorated" with masses or rigid disks, have been shown to selectively absorb low-frequency sound.[3–8] Counterintuitively, Yang *et al.*[3] demonstrated that such a structure could break the mass-density law of sound attenuation[9] by a factor of 200, a consequence of the structure's effective negative dynamic mass characteristics, arising from the multiple low-frequency vibrational eigenmodes of the system. In a similar structure, Mei *et al.*[8] reported almost unity absorption at certain frequencies, where the structure was described to be acoustically "dark," the minimal coupling of the flapping motion of the metal platelets to radiative modes explained this behaviour. Further advances in the field were reported by Ma *et al.*[10] who experimentally observed an extremely sharp absorption peak with an absorption coefficient >0.99 (implying a near-perfect impedance match with air) attributable to the excitation of hybridised resonances supported by an acoustic membrane-type metasurface.

A two dimensional plate-type acoustic metamaterial, consisting of a periodic arrangement of cylinders, composed of a layer of tungsten and a layer of silicon, deposited on a thin aluminium plate, has been presented as an experimental realisation of an effective, yet not bulky, broadband acoustic metamaterial for low-frequency sound attenuation.[11] As a result of the resonance of the cylinders, a broad band-gap is observed in the transmission associated with the out-of-plane plate modes, at frequencies where the wavelength in air is approximately three orders of magnitude larger than the plate thickness. Furthermore, an omni-directional broadband acoustic absorber of airborne sound, the acoustic analogue of the optical black-hole,[12] has been demonstrated experimentally.[13] In this study, Climente *et al.* utilised a graded index (GRIN) structure to guide the sound energy towards a lossy core, where 80% of the impinging acoustic energy was shown to be dissipated.

More recent advancements in the exploitation of acoustic metamaterial structures to attenuate airborne sound include the works of Christensen *et al.*,[14,15] who explored anisotropic porous lamella structures and how stochastic variations of their effective parameters could lead to increased absorption of sound. Established principles from the electromagnetic domain have also been applied in the acoustic domain, for instance, in the work of Wei *et al.*[16] Here, the concept of coherent perfect absorption (CPA), originally proposed in the optical domain by Chong *et al.*[17] as the time-reversed counterpart of a laser that fully absorbs incoming coherent light with a specific set of relative phases and intensities, is extended into the domain of acoustic waves. A sound absorbing panel, which utilises coiled cavities that act as Helmholtz resonant chambers to reduce the thickness of the panel, has also been proposed in the experimental study by Cai *et al.*[18] Another recent study demonstrates a metamaterial, comprising multiple acoustic labyrinthine resonators and foam absorber, with near-unity broadband sound absorption achieved by the interaction of evanescent fields with an absorber material.[19]

Here, we report the remarkable absorption properties, on resonance, of an acoustic metamaterial structure of subwavelength thickness that comprises a perforated plate, separated from a rigid boundary by a deeply subwavelength narrow channel of air. This simple, easily fabricated, robust structure is an ideal candidate for a sound absorbing panel, characterised by an experimentally observed near 100% deep minimum in specular reflectance at selective frequencies, achieved through thermo-viscous loss and tuned by the air channel thickness.

The experimental sample comprises two aluminium plates, which are assumed to be perfectly rigid. The top plate

a)t.a.starkey@exeter.ac.uk

of mean thickness $L = 5.07$ mm extends approximately 450.0 mm in both the x- and y- directions and is perforated by a square array of open circular holes (pipes) with radius $r = 4.4$ mm and pitch $P = 16.5$ mm. A photograph of this plate is shown in Figure 1. The perforated plate is separated from an untextured flat base plate by an air layer (narrow channel) of thickness g. Experimentally, the separation of the two plates, g, is achieved by uniformly distributing twelve 10.0 mm square Mylar® spacers, of the desired thickness, between the two plates. A schematic representation of the structure's unit cell is shown as an inset in Figure 1, where the grey shaded geometry represents the sound hard material.

The near-normal incidence specular reflectance (reflectance, R), from the entire panel as a function of frequency, for different values of g, is obtained experimentally using a pulse-measurement technique in a free-space environment. The experimental set-up comprises an acoustic source (Scan-Speak R3004/602010 tweeter) and a microphone (constructed using an electret condenser microphone cartridge (Panasonic WM-61A)), placed side by side, at the focal plane of a spherical aluminium mirror. The mirror collimates the beam, such that a close to plane wave pressure field is incident near-normal upon the sample. Upon set-up, the mirror is rotated such that the reflected beam gives a maximum signal at the microphone detector. An aperture, formed from the sound absorbing material, surrounds the sample to reduce scattering from the edge of the finite sample. In order to obtain the reflectance from the sample, first the magnitude of the Fast Fourier Transform (FFT) of the detected pulse with the sample present is normalised using the magnitude of the FFT of a reference signal taken when the sample is replaced by a flat rigid plate, and then the absolute value is squared. The experimental data are directly compared to numerical simulations obtained using COMSOL Multiphysics 5.2a (which simulates the response of the structure to a normally incident plane wave), and excellent agreement is shown. In the numerical simulations, both viscous and thermal loss contributions are considered due to their significant effect in narrow cavities,[20] and literature values for the velocity of sound were used[21] in order to replicate the measurement environments.

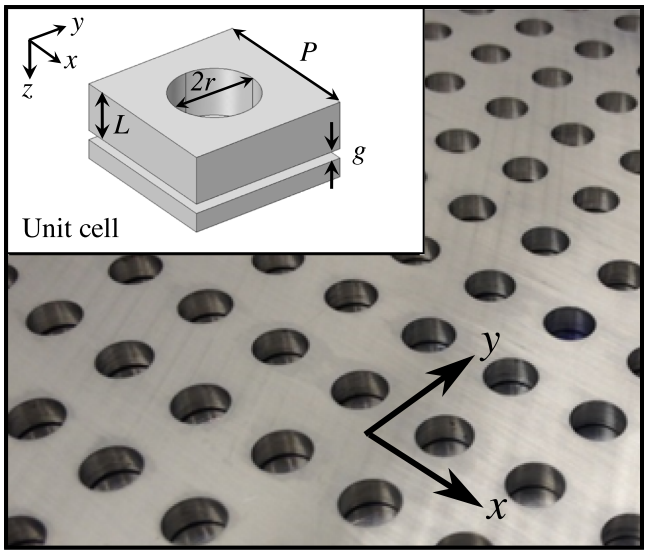

FIG. 1. Photograph of the top perforated plate of the experimental sample. Inset: schematic representation of the sample unit cell (not to scale) with pitch, P. The plate perforations are pipes of radius r and length L. The thickness of the channel of air, g, is defined as the separation of the two plates. The co-ordinate system is shown.

It is important to notice that the diffraction edge, defined by the sample pitch in the x- and y- directions, occurs at ≈21 kHz. Therefore, in the frequency range considered here (8–18 kHz), the sample is non-diffracting; and in the absence of transmission through the sample all incident sound is either reflected in the specular direction or attenuated ($A = 1 - R$).

Initially, the normal-incidence reflectance from the sample with no gap present between the two plates ($g = 0$), i.e., an array of close-ended holes, is numerically modelled; a very broad shallow (≈11% deep) minimum in the reflectance is observed at 12.6 kHz (pink dashed curve in Fig. 2). This minimum corresponds to the frequency at which the lowest order standing wave resonance is supported by each hole, i.e., where the pressure field is maximum at the bottom of the hole and zero close to the entrance of the hole (not shown). To compare with these results, experimental data were obtained with no spacers present between the two plates (blue solid curve in Fig. 2). However, this shows a strong resonance, and best agreement with these data is shown when a value of $g = 60\ \mu$m is used in the simulations (blue dotted curve in Fig. 2). This result is attributed to air gaps arising from the flatness tolerance of the perforated plate above the rigid boundary, which is caused during the fabrication process.

As the gap between the plates increases, the system moves towards the optimum coupling condition (i.e., 100% deep minimum in reflectance). When 50 μm thick polyester spacers are placed between the two plates, a deep minimum in the specular reflectance is observed (red solid curve in Fig. 2); at the resonance, there is an approximate 9-fold reduction in the reflectance from the sample, compared to that predicted when no gap is present between the two plates. Note that excellent agreement with the experimental data is obtained with a fitted value of $g = 85\ \mu$m, as indicated by the red dotted curve in Figure 2.

The optimum coupling condition (i.e., 100% deep minimum in reflectance) is achieved when the radiative and non-radiative losses in the system are balanced. Upon introducing a gap between the two plates, a narrow channel of air is introduced that is bound largely by acoustically rigid walls,

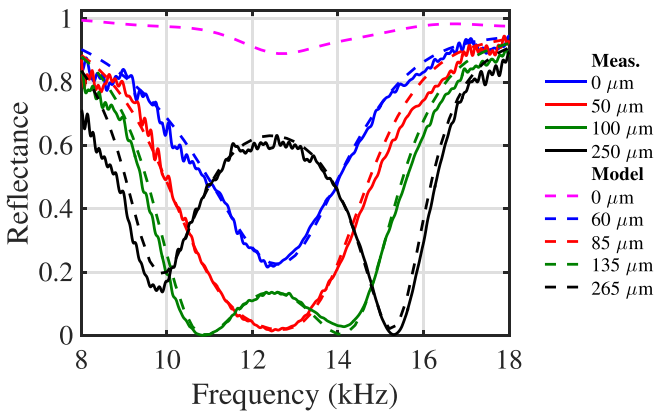

FIG. 2. Measured (solid lines) and numerically modelled (dotted lines) normal incidence reflectance spectrum for different values of the thickness of the channel of air between the two plates, g.

at which the "no-slip" boundary forces the tangential particle velocity to zero. This exerts a frictional shear force on the overlying fluid and a viscous boundary layer is formed (of characteristic length $\delta_v \approx \sqrt{\frac{\nu}{\omega}}$, where ν is the coefficient of shear viscosity). Simultaneously, thermal conduction allows heat transfer to take place between the fluid (air) and the walls, and a thermal boundary layer is formed (of characteristic length $\delta_\kappa \approx \sqrt{\frac{\kappa}{\omega}}$, where κ is the thermal conductivity).[22] The losses associated with these boundary layers (with thicknesses on the order of tens of microns at these frequencies) are advantageously used to tune the absorption in the system, by varying the thickness of the gap between the two plates, such that a close-to 100% deep minimum in reflectance can be obtained.

Two modes are resolved in the reflectance spectrum upon further increasing the gap between the two plates; the solid green and black curves in Figure 2 show the normal incidence reflectance spectrum when spacers of thickness 100 μm and 250 μm, respectively, are placed between the two plates. It can be seen from Figure 2 that the lowest frequency resonance moves down in frequency with increasing gap size, whilst the highest frequency resonance moves up in frequency as g is increased. Numerical simulations reveal that a value for $g = 135\,\mu$m (green dotted curve) gives best agreement to the experimental data when spacers of thickness 100 μm are placed between the two plates. A least squares fit is used to determine that a simulated value of $g = 265\,\mu$m (black dotted curve in Fig. 2) provides the best agreement to the data when 250 μm thick spacers are used. Simulated reflectance for increasing incident angle also show that for each gap size considered, the spectral position and absorption minima remain comparable before the onset of diffraction (see Supplementary Material).

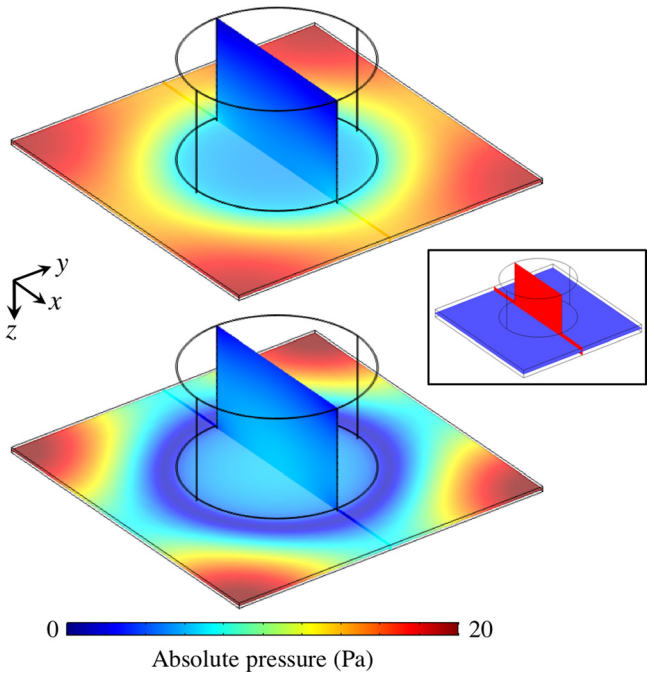

FIG. 3. Pressure amplitude field profiles, for $g = 265\,\mu$m, plotted on the xy-plane at the mid-height between the two plates (blue plane inset) and on the xz-plane at the centre of the cavity (red plane inset). Top: lowest frequency minimum in reflectance (9.8 kHz). Bottom: highest frequency minimum in reflectance (15.3 kHz). Red regions correspond to high pressure field and blue to zero pressure.

The numerical model is utilised to explore the pressure field profiles on resonance, in order to gain a deeper understanding of the behaviour of the system. Figure 3 shows the pressure field amplitudes, when $g = 265\,\mu$m, plotted in the xy-plane at the mid-height of the channel of air between the two plates and the xz-plane at the centre of the cavity, for both reflectance minima. Figure 3 displays the distribution of the pressure field amplitude for the lower frequency resonant minima (9.8 kHz) and the higher frequency resonance (at 15.3 kHz), in the top and bottom schematic, respectively. It can be seen that for the lowest frequency mode f_1 (Fig. 3 (top)), strong fields (red regions) are localised within the gap between the two plates, falling to zero along the length of the hole, with a pressure minimum (indicated by blue regions) observed close to the entrance of the hole, i.e., an approximate quarter wavelength resonance is supported by the entire cavity. For the higher frequency mode f_2, as seen in Figure 3 (bottom), *two* pressure nodes (blue regions) are observed in the resonant fields, one within the gap between the two plates and one close to the entrance of the hole, i.e., an approximate three-quarters wavelength resonance is supported by the entire cavity.

Further insight into the behaviour of the system can be obtained by examining the amplitude of the pressure field within the channel of air between the plates, for different values of g. Figure 4 shows the amplitude of the pressure field, evaluated along the intersection of the air gap mid-height xy-plane with the mid-pipe xz-plane (planes depicted in Fig. 3 (inset)) for (a) $g = 265\,\mu$m, (b) $g = 135\,\mu$m, (c) $g = 85\,\mu$m, and (d) $g = 60\,\mu$m. In Figures 4(a) and 4(b), the solid blue and dotted blue curves correspond to the frequency of the lowest (f_1) and highest (f_2) order resonances, respectively, and the solid blue lines in Figures 4(c) and 4(d) indicate the frequency of the single resonance supported by the structure. The dashed lines indicate the position of the edge of the pipe. Whilst it can be seen that for each resonance the maximum pressure fields are observed at the edge of the unit cell, a minimum in the pressure field is observed close to the edge of the pipe only for each of the higher order modes (blue dotted curves Figs. 4(a) and 4(b)). This pressure minimum becomes less pronounced as the gap is reduced, as f_1 and f_2 become closer together in frequency. For the two smallest gap sizes,

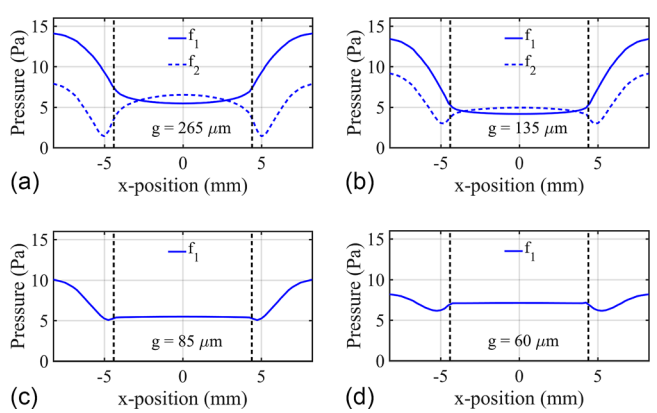

FIG. 4. Predicted pressure amplitudes evaluated along the intersection of the xy- and xz- planes as shown in the inset in Fig. 3, for (a) $g = 265\,\mu$m, (b) $g = 135\,\mu$m, (c) $g = 85\,\mu$m, and (d) $g = 60\,\mu$m. Pressure amplitudes for frequency of the lowest (f_1) and highest (f_2) order resonances, respectively, in (a) and (b) and the frequency of the single resonance supported by the structure in (c) and (d). (Black dashed lines indicate the position of the edge of the pipe.)

$g = 85\,\mu$m and $g = 60\,\mu$m, when only a single resonance (reflectance minimum) is observed, the pressure field profiles (Figs. 4(c) and 4(d)) have a mixed character of the two individual resonances observed for the larger gap sizes.

In conclusion, we report on the experimental investigation of an acoustic metamaterial structure for the attenuation of low-frequency airborne sound, which comprises a perforated plate separated from a rigid boundary by a deeply subwavelength narrow channel of air. The results obtained demonstrate the ability to control the attenuation properties of the system via the thickness of this channel, with near unity absorption, experimentally observed as >99% deep reflectance minima, reported for certain air gap sizes. The remarkable increase in absorption, compared to when no gap is present between the two plates, is attributed to the increase in the non-radiative losses in the system due to the thermo-viscous losses within the thin layer of air on the inner surfaces of the subwavelength channel. Excellent agreement with numerical simulations is shown. This simple, robust, and easily fabricated structure, with easily tuneable absorption properties, has potential for noise control applications. Sound absorber panels designed incorporating a distribution of different periodicities, air gap thicknesses, and textured base plates maybe used to enhance losses across the frequency range to realise broadband absorption using sound hard materials.

See supplementary material for numerical analysis of reflectance as a function of incident angle.

The authors wish to acknowledge financial support from DSTL and QinetiQ.

[1]J. P. Arenas and M. J. Crocker, J. Sound Vib. **44**, 12 (2010).
[2]D.-Y. Maa, J. Acoust. Soc. Am. **104**, 2861 (1998).
[3]Z. Yang, J. Mei, M. Yang, N. H. Chan, and P. Sheng, Phys. Rev. Lett. **101**, 204301 (2008).
[4]S. H. Lee, C. M. Park, Y. M. Seo, Z. G. Wang, and C. K. Kim, Phys. Lett. A. **373**, 4464 (2009).
[5]Z. Yang, H. M. Dai, N. H. Chan, G. C. Ma, and P. Sheng, Appl. Phys. Lett. **96**, 041906 (2010).
[6]C. J. Naify, C.-M. Chang, G. McKnight, and S. Nutt, J. Appl. Phys. **108**, 114905 (2010).
[7]C. J. Naify, C.-M. Chang, G. McKnight, F. Scheulen, and S. Nutt, J. Appl. Phys. **109**, 104902 (2011).
[8]J. Mei, G. Ma, M. Yang, Z. Yang, W. Wen, and P. Sheng, Nat. Commun. **3**, 756 (2012).
[9]Z. Liu, X. Zhang, Y. Mao, Y. Y. Zhu, Z. Yang, C. T. Chan, and P. Sheng, Science **289**, 1734 (2000).
[10]G. Ma, M. Yang, S. Xiao, Z. Yang, and P. Sheng, Nat. Mater. **13**, 873 (2014).
[11]M. Badreddine Assouar, M. Senesi, M. Oudich, M. Ruzzene, and Z. Hou, Appl. Phys. Lett. **101**, 173505 (2012).
[12]E. E. Narimanov and A. V. Kildishev, Appl. Phys. Lett. **95**, 041106 (2009).
[13]A. Climente, D. Torrent, and J. Sánchez-Dehesa, Appl. Phys. Lett. **100**, 144103 (2012).
[14]J. Christensen, V. Romero-García, R. Picó, A. Cebrecos, F. J. G. de Abajo, N. A. Mortensen, M. Willatzen, and V. J. Sánchez-Morcillo, Sci. Rep. **4**, 4674 (2014).
[15]J. Christensen and M. Willatzen, Appl. Phys. Lett. **105**, 043508 (2014).
[16]P. Wei, C. Croënne, S. Tak Chu, and J. Li, Appl. Phys. Lett. **104**, 121902 (2014).
[17]Y. D. Chong, L. Ge, H. Cao, and A. D. Stone, Phys. Rev. Lett. **105**, 053901 (2010).
[18]X. Cai, Q. Guo, G. Hu, and J. Yang, Appl. Phys. Lett. **105**, 121901 (2014).
[19]M. Yang, S. Chen, C. Fu, and P. Sheng, e-print arXiv:1609.09561.
[20]G. P. Ward, R. K. Lovelock, A. R. J. Murray, A. P. Hibbins, J. R. Sambles, and J. D. Smith, Phys. Rev. Lett. **115**, 044302 (2015).
[21]O. Cramer, J. Acoust. Soc. Am. **93**, 2510 (1993).
[22]L. E. Kinsler, A. R. Frey, A. B. Coppens, and J. V. Sanders, *Fundamentals of Acoustics*, 4th ed. (Wiley, NY, 1999).